

The Applicability of Rock Bolt Supporting Factor based on Rock Mass Behavior: A Case Study of Alborz Tunnel

Hamed Farajollahi¹, Mohammad Mohammadi², and Mohammad Hossein Khosravi^{3*}

1. School of Mining Engineering, College of Engineering, University of Tehran, Tehran, Iran

2. Division of Soil and Rock Mechanics, KTH Royal Institute of Technology, Stockholm, Sweden

3. Department of Mining Engineering, Faculty of Engineering, University of Birjand, Birjand, Iran

Article Info

Received 8 April 2024

Received in Revised form 30 July 2024

Accepted 25 August 2024

Published online 30 August 2024

DOI: [10.22044/jme.2024.14405.2697](https://doi.org/10.22044/jme.2024.14405.2697)

Keywords

Rock mass behavior

GDE multiple graph

Rock Mass Rating system (RMR)

Rock Bolt Supporting Factor (RSF)

Alborz tunnel

Abstract

A better understanding of rock mass behavior is an essential part of the design and construction of underground structures. Any improvement in the understanding of the behavior of rock mass will facilitate the improvement of the design in terms of the safety of the working environment, long-term safety of the structure, environmental effects, and sound management of public or private resources. Thus, in step one in this paper the experience gained from applying the GDE (Geo Data Engineering) multiple graph approach for rock mass classification and assessing its behavior throughout excavation of the Alborz tunnel is presented. The predicted hazards are compared with the experienced problems and suggestions are given to be considered in future works of tunnel construction. In step two, the GDE multiple graph approach is compared to the rock mass behavior types proposed by Palmstrom & Stille (2007) in terms of the continuity of rock mass. The result of this comparison together with the data obtained from rock mass classification in the Alborz tunnel are used to develop a system that determines the applicability of the rock bolt supporting factor (RSF) in different rock mass behavior classes.

1. Introduction

The three main preliminary design methods of underground structures in rock engineering are analytical, observational, and empirical approaches [1]. The rock mass classification systems constitute the backbone of commonly used empirical methods, and provide valuable aid for systematic design of underground structures. The most important classification systems include Terzaghi's classification, the stand-up time classification, the Rock Quality Designation (RQD), the Rock Structure Rating (RSR), the Rock Mass Rating (RMR), the Q system, the Geological Strength Index (GSI), and Rock Mass index (RMi) [1–10]. Further development of these classifications includes the quantitative GSI chart for characterization of poor and very poor rock masses, the modified GSI system for tectonically disturbed heterogeneous rock masses, the Mining

Rock Mass Rating (MRMR), the Rock Mass Quality Rating (RMQR), the Anisotropic Rock Mass Rating (ARMR), the Directional Rock Mass Rating (DRMR), the adjusted RMR for underground intersections, the Q-slope system, and the Q-slope system for faulted rocks and fault zones [11–20]. Some researchers have also used the combined methods of RMR and Q systems and have developed the relationships presented between these two systems with the aim of localization and obtaining better results [21].

Classification systems are useful tools for both the design and construction stages of underground structures. However, these systems have their shortcomings such as limited applicability in weakness zones [22]. Moreover, it is the behavior of the surrounding rock mass in interaction with the underground structure that is crucially important

✉ Corresponding author: mh.khosravi@birjand.ac.ir (M.H. Khosravi)

and needs to be understood well. This issue has been investigated mainly by Palmstrom and Stille [22–24]. The “GDE multiple graph” approach describes the behavior of rock mass surrounding an underground structure by incorporating the GSI, R_{Mi} (block volume) and RMR classifications together with the effect of the intact rock strength and stress condition [25, 26, 28].

A new concept about the rock bolting capability of rock mass was introduced by Mohammadi et al., which is based on the RMR system [29]. This concept is called rock bolt supporting factor (RSF) and can be used to determine the efficiency of rock bolting in a given rock mass, which can be a useful tool in empirical design of underground structures in rock. One of the applications of the RSF for determining the RMR value of rock masses consisting of alternate weak and hard rock layers is demonstrated by Mohammadi and Hossaini [30]. However, in the original paper by Mohammadi et al. [29], the range of applicability of the RSF is not specified, meaning that it is not clear that in which types of rock mass behavior the RSF concept is valid.

Thus, the objectives of this paper are two-fold. First, the experience obtained from the application of the GDE multiple graph during the construction of the 6.4 km long Alborz tunnel is presented and the real outcomes in terms of hazards are compared with the predicted possible hazards by the multiple graph method. Then the principle categories of rock mass behavior based on the GDE multiple graph approach are compared with those published by Palmstrom and Stille [22], which henceforth is referred to as GBT approach (Ground Behavior Types). This comparison coupled with analyzing the data obtained from the construction of the Alborz tunnel pave the way for determining the range of applicability of the RSF concept, which is the second objective of the paper. Thus, in section 2 the GDE and GBT approaches are presented. In sections 3 the RSF concept is described, and section 4 presents the Alborz tunnel. In section 5, the application of the GDE multiple graph approach in the construction phase of the Alborz eastern main tunnel together with the suggestions on the issues to be considered for the design and construction of tunnels using the GDE multiple graph method are put forward. The applicability of the RSF is discussed in section 6 and finally in section 7 where the conclusions are presented.

2. Rock mass behavior

2.1. The GDE multiple graph approach

The GDE multiple graph approach is a method for preliminary assessment of surrounding rock mass behavior in tunnel excavation [25–27]. This method can also be used to select the support class to install at the tunnel face based on pre-defined design criteria [31–35]. The GDE multiple graph is consisted of four graphs representing rock mass fabric, rock mass strength, competency, and excavation behavior, respectively (Figure 1). These graphs are defined by Russo [28]:

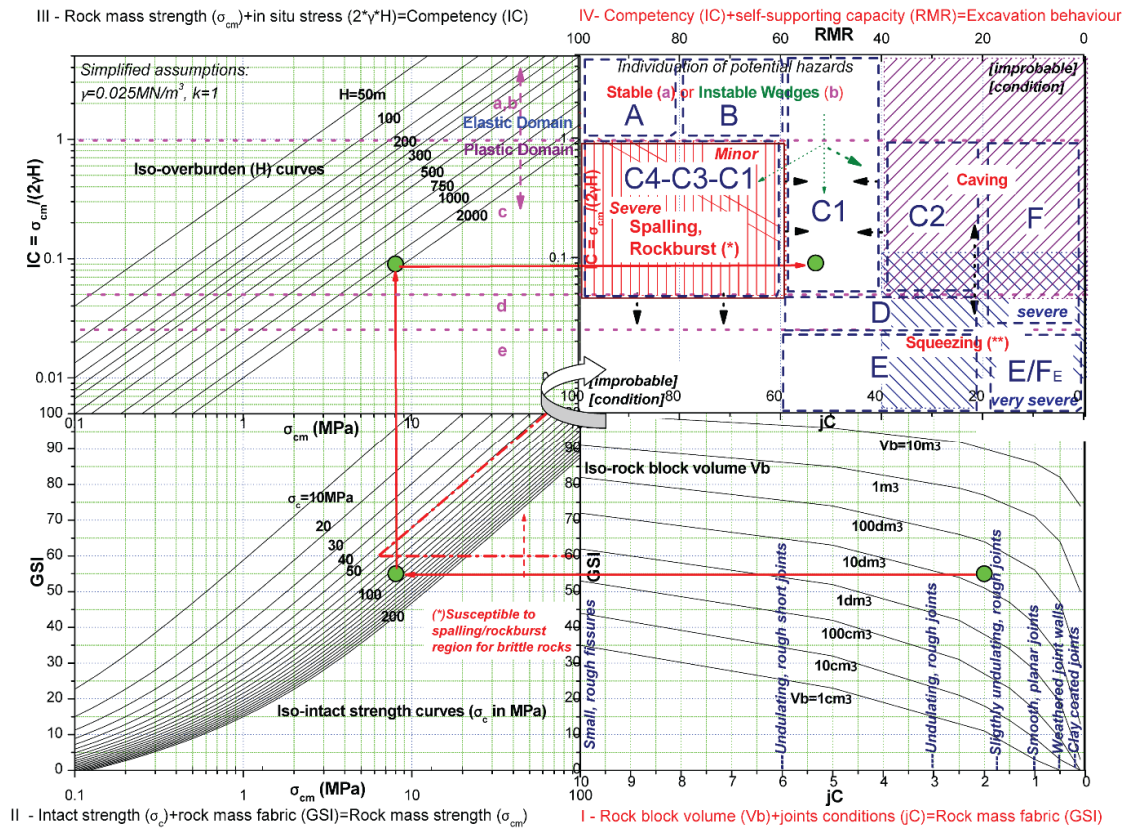
- The rock mass fabric (GSI) represents the rock block volume (V_b) and joints condition (jC), which is shown in the lower-right side of Figure 1.
- The rock mass strength (σ_{cm}) is represented by the intact rock strength (σ_c) and rock mass fabric (GSI), which is shown in the lower-left side of Figure 1.
- Competency (IC) is the combined effect of rock mass strength (σ_{cm}) and in-situ stress:

$$IC = \sigma_{cm}/2\gamma H \quad (1)$$

where γ is the unit weight of the rock mass which is assumed to be 0.025 MN/m³ in a hydrostatic stress condition ($k=1$), and H represents the overburden. The GDE geotechnical condition are defined based on the range of IC which are: a/b , c , d , and e . For a/b the IC is above 1 where the elastic behavior of the rock mass is expected. For c , d , and e the ranges of IC are 0.05-1, 0.025-0.05, and 0-0.025, respectively, all of which constitute the plastic domain. This is demonstrated in the upper-left side of Figure 1.

- Excavation behavior is represented by the competency (IC) and the rock mass rating (RMR). The behavior of rock mass is classified into 6 groups: A, B, C, D, E, and F. The C group is further subdivided into 4 sub-groups: C1, C2, C3, and C4, where C1 has two components in which the RMR range is different (see the upper-right side of Figure 1).

The GDE multiple graph approach can be used to identify potential hazards of tunneling in order to plan suitable mitigating measures during the planning phase as well as selection of support system to be installed at tunnel face during construction phase. The possible ground behavior types based on the GDE multiple graph approach are presented in Table 1.



III - Rock mass strength (σ_{cm}) + in situ stress ($2 \cdot \gamma \cdot H$) = Competency (IC) IV - Competency (IC) + self-supporting capacity (RMR) = Excavation behaviour
 II - Intact strength (σ_c) + rock mass fabric (GSI) = Rock mass strength (σ_{cm}) I - Rock block volume (V_b) + joints conditions (jC) = Rock mass fabric (GSI)
 (*) only for the susceptible region, otherwise the development of plastic region and moderate radial convergences are more probable
 (**) depending also from the length of the potential pruned zone: given a possible "silo effect", for short zones included in good quality rocks, a caving behaviour it is most likely

Figure 1 An example of the GDE multiple graph [28]

Table 1. Ground behavior types based on the GDE multiple graph approach (modified after Russo [28])

| Geotechnical condition | | Prevalent hazard | Cause | Section type | Ground behavior |
|------------------------|-----------------|------------------------------------|---------------------|--------------|--|
| GDE | RMR | | | | |
| A | I | Wedge instability/ Rock fall | Gravity | A | Stable rock mass, elastic response, possible local rock fall |
| B | II | | | B | Elastic response, wedge instability |
| C | III | | | C1 | Rock fall, possibility of moderate development of plastic zone |
| C | I, II | Spalling/ Rock burst | Stress | C1 | Mild brittle failure, minor block ejection, minor spalling/rock burst |
| C | I, II | | | C3 | Sudden brittle failure, moderate spalling/rock burst |
| C | I, II | | | C4 | Sudden violent brittle failure, severe spalling, heavy rock burst |
| D | III, IV, (V) | Plastic deformations/ Squeezing | Stress | D | Plastic deformations, tunnel face extrusion, and radial convergences (→severe squeezing) |
| E | | | | E | Intense plastic deformations, large extrusion of tunnel face, and radial convergences (→very severe squeezing) |
| C | IV | Caving/ Flowing ground | Gravity (and water) | C2 | Gravity-driven instability, moderate development of plastic zone |
| (e)/f | V | | | F/FE | Sever gravity-driven instability, immediate collapse of tunnel face and contour, includes flowing ground |

2.2. Ground Behavior Types (GBT)

The behavior of the rock mass around an underground opening is usually affected by several factors. These factors include the rock mass structure, the continuity factor of the rock mass, the state of stress around the opening, the time, the presence of water, and the way the particles and

blocks move around the opening [24]. Recognizing and categorizing the rock mass behavior is essential in order to properly predict the probable hazards that can be encountered during the construction of an underground structure, design a suitable support system, and ensure the safety of the workers and the engineering structure. The parameters that govern the ground behavior around

an underground opening are the ground condition and project-related features. Factors related to the former category are rock mass composition, the effect of stresses, and groundwater condition. The latter includes parameters such as the opening dimensions, shape, and method of excavation.

Thus, as a result of the combined effect of these factors various types of rock mass behavior may take place (Table 2). Moreover, in a certain part of an underground structure, one or several types of rock mass behavior can occur.

Table 2. Main ground behavior types in underground excavations (modified after Palmstrom and Stille [22])

| Ground behavior | Continuity | Comments |
|-----------------------------|----------------------------|---|
| Gravity driven | | |
| Stable | Continuous | Massive rocks at low and moderate depths |
| Block falls | Discontinuous | Stable with possibility of block failure |
| Cave-in | Continuous | Highly jointed or crushed rock |
| Running ground | Continuous | Coarse sands and gravels above ground water level |
| Stress-induced behavior | | |
| Buckling | Discontinuous | Anisotropic, hard, brittle rock under high load |
| Slabbing | Continuous | Overstressing of massive hard, brittle rock |
| Rock burst | Continuous | Very high overstressing of massive hard, brittle rock |
| Rupturing from stresses | Continuous | Time-dependent effect of slabbing or rock burst |
| Initial plastic deformation | Continuous | Due to overstressing in deformable rock |
| Squeezing | Continuous | Overstressing of plastic, massive rocks and materials |
| Water-influenced | | |
| Ravelling from slaking | Continuous - Discontinuous | Disintegration of some coherent and friable materials |
| Swelling | Continuous | Swellings of certain rocks or clay minerals |
| Flowing ground | Continuous | Particulate materials with low coherence |
| Water ingress | | |

3. Rock bolt supporting factor (RSF)

The condition of discontinuities is an important parameter of the RMR system which constitutes 30 points out of 100 points of this system. The parameter itself includes 5 characteristics of discontinuities, i.e. persistence, aperture, roughness of joint surfaces, type of infilling material, and degree of weathering in the joint surfaces. These characteristics contribute to the RMR rating based on the degree of their effect on improving shear resistance of discontinuity surfaces.

A sufficiently well-designed rock bolt supporting system would prevent the rock blocks from falling, sliding, and rotation through increasing the shear resistance of the discontinuity surfaces. In fact, in such a system, the aforementioned characteristics of discontinuities are not eliminated, but the shear resistance of the discontinuity surfaces can be assumed to have been increased. Accordingly, the combination of the rock mass and bolts can be considered as an equivalent rock mass having a higher rating for condition of discontinuities. This notion, is the basis of the rock bolt supporting factor (RSF) representing the rock bolting capability of a given rock mass. Thus, RSF can be calculated as below [29]:

$$RSF = [100 - 10 \times r_{co}/3] \quad (2)$$

where r_{co} is the total rating for condition of discontinuities in the RMR system.

The RSF is a property of rock mass and its value represents the capability of the rock mass to be improved by rock bolting. The higher values of RSF indicate the higher capability of rock mass to be enhanced by rock bolting. The magnitude of enhancement can be formulated by definition of RMR_{eq} which is the RMR value of the rock mass where the total rating for condition of discontinuities is assumed to be at its maximum, i.e. 30, which represents the rock mass reinforced by rock bolts [29]:

$$RMR_{eq} = RMR + 0.3RSF \quad (3)$$

The mechanism behind rock bolting remains not completely understood because of the diverse properties of bolts and rocks. Habenicht (1983) examined four scenarios to clarify some key bearing capacity mechanisms associated with rock bolting [36]. These scenarios include suspending, nailing, beam building, and arch building effects. A properly designed rock bolting system must satisfy specific criteria based on at least one of these four effects. In certain complex situations, multiple effects may be taken into account. Building on the concept of reinforcement through rock bolting, a fifth principle of bolting can be

proposed. As discussed above, this principle is quite straightforward: rock bolting enhances the discontinuity rating to its peak within the RMR system, leading to the assumption that the RMR value of a rock mass also rises [29].

Equation 3 provides the mathematical definition of the fifth principle of rock bolting, and its significance lies in its presentation as a mathematical equation rather than merely an explanatory statement. It is important to note that any decimal value calculated for $RMReq$ should be rounded up to determine the precise value of $RMReq$, as the mathematical $\lceil \cdot \rceil$ sign was employed to derive the value of RSF [29].

4. The Alborz tunnel

The Alborz tunnel, with an approximate length of 6.4 km, is part of the Tehran-Shomal freeway project, which connects the capital city of Tehran to the city of Chalous on the coastal area of the

Caspian Sea. The Alborz tunnel project is consisted of two main tunnels (known as eastern and western tubes) which have an approximate distance of 80 m from each other as well as one exploratory tunnel in between them (Figure 2). The main tunnels and the exploratory tunnels are connected to each other by cross passage tunnels. The exploratory tunnel was excavated by using an open-shield TBM with the diameter of 5.2 m in order to obtain full geological information along the tunnel route. This tunnel is planned to be used as an escape tunnel during the emergencies when the main tunnels are in operation. The eastern tunnel is also excavated using drill and blast method while the excavation of the western tunnel has recently started by drill and blast method. Based on the information obtained from the excavation of exploratory and eastern tunnels the entire length of the tunnels were divided into 7 geological zones which are described in Table 3.

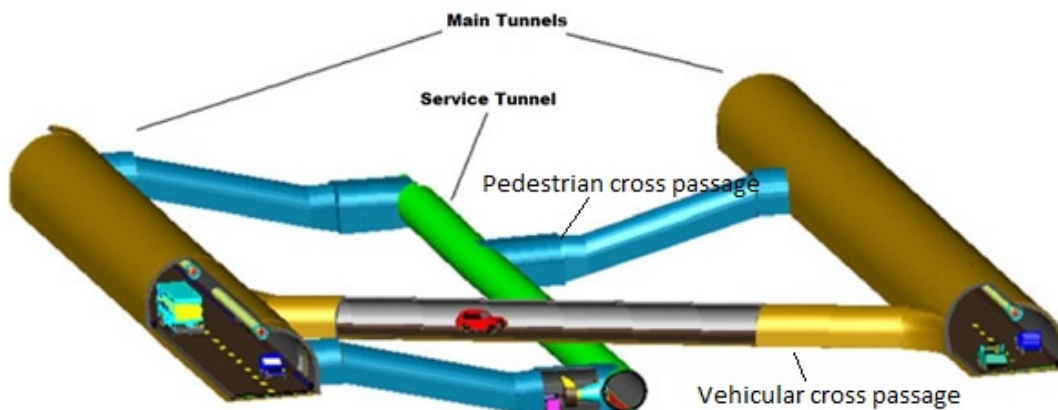


Figure 2. Schematic overview of the Alborz Tunnel

Table 3. The encountered geological conditions along the Alborz tunnel route [37]

| Zone | Formation | Total length (m) | Lithology |
|------|--------------------|------------------|--|
| 1 | Karaj | 1000 | Sequences of grey tuff, sandstone, limestone, and andesite |
| 2 | Karaj | 500 | Anhydrite with occasional interbedding of black tuff |
| 3 | Karaj | 950 | Interbedding of grey and black tuff |
| 4 | Karaj | 530 | Gypsum with lenses of black tuff |
| 5 | Kandevan fault | 400 | Fault gouge with fragments of tuff, anhydrite, and andesite |
| 6 | Doroud formation | 470 | Sequences of sandstone and limestone with occasional occurrence of dacitic dykes |
| 7 | Shemshak formation | 2550 | Sequences of argillaceous shale, sandstone, and siltstone with occasional occurrence of coal seams and dacitic dykes |

The surrounding rock mass in the area is highly tectonized with numerous occurrences of fault zones with the impact zones varying from 0.5 m up to 10 m. In many parts of the tunnel the folding of the beddings are observed and numerous joint sets occur in most of the geological zones. The

minimum overburden of 40 m occurs in the portals of the tunnel and gradually increases to the maximum of 850 m in the middle of the tunnel. The eastern tunnel was designed based on the geological information obtained from the excavation of the exploratory tunnel using the GDE

multiple graph approach. The GDE multiple graph approach was used during the construction phase to select the suitable primary support after each blasting round. The excavation method as well as

the required primary support system suggested by the GDE multiple graph approach for the construction of the Alborz eastern tunnel are presented in Table 4.

Table 4. The excavation method and primary support system in each ground class in the Alborz eastern tunnel (Technical Report, 2015)

| Ground class | Excavation method ^a | Primary support details |
|-------------------|--|--|
| B | Top and bench (advance: 3.5 m) or full face | Mechanically anchored bolts: L=4.5 m, spacing: 2.5 (±0.5)*2.5 (±0.5) Wiremesh + Shotcrete (5 cm) |
| C1 (RMR=40-60) | Top and bench (advance: 2.5 m) | Mechanically anchored bolts: L=4.5 m, spacing: 1.5 (±0.25)*1.5 (±0.25) One layer of wiremesh + two layers of shotcrete (15 cm) |
| C2 | Top and bench (advance: 1.25 m) | Spiling (if required) Fully grouted bolts: L=4.5 m, spacing: 1.25 (±0.25)*1.25 (±0.25) Two layers of wiremesh + lattice girder with 3 bars + three layers of shotcrete (25 cm) |
| D | Top and bench (advance: 1.25 m – 10-15 cm over-excavation) | Fully bonded fiber glass elements at face (L=12 m, Number=32) Fully grouted bolts: L=6 m, spacing: 1.25 (±0.25)*1.25 (±0.25) Two layers of wiremesh + sliding steel rib TH44 + three layers of shotcrete (30 cm) Temporary invert (20 cm shotcrete + one layer of wiremesh) |
| E | Top and bench (advance: 1.25 m – 10-15 cm over-excavation) | Fully bonded fiber glass elements at face (L=12 m, Number=41) Fully grouted bolts: L=6 m, spacing: 1 (±0.25)*1 (±0.25) Two layers of wiremesh + sliding steel rib TH44 + three layers of shotcrete (35 cm) Temporary invert (20 cm shotcrete + one layer of wiremesh) |
| F | Top and bench (advance: 1.25 m) | Spiling (L=4 m, spacing=0.8 m, fully grouted) Fully grouted bolts: L=4.5 m, spacing: 1.25 (±0.25)*1.25 (±0.25) Two layers of wiremesh + lattice girder with 3 bars + three layers of shotcrete (25 cm) |

^a In all rock types 4 drainage pipes with a length of 30 m and overlap of 10 m, and diameter of 51 mm (2") are suggested if ground water is present.

5. The application of GDE multiple graph

5.1. Experience from the excavation of the Alborz tunnel

The geological condition and observed behavior of the rock mass during the excavation of the Alborz eastern tunnel per each zone of Table 3 are shown in table 5. The experience from the excavation of the Alborz tunnel shows that the GDE multiple graph approach can be a reliable tool for both the design and construction of tunnels. The followings are the highlights of the experience from the Alborz exploratory and eastern tunnels regarding the rock mass behavior:

Type C1: All the C1 types encountered in the Alborz tunnel belong to the RMR class III (see Figure 1). The rock fall/wedge instability was observed in all cases. It was observed that the rock mass behavior is highly dependent on the joint orientation with regard to the tunnel axis. When the prevailing joint sets have a strike parallel to the tunnel axis, and the dip angle between 20 and 45 degrees (see Wickham et al. [10]) the occurrence of overbreak in one of the tunnel walls is inevitable. In such cases, it is recommended to use spiling in one side of the tunnel wall (depending on the dip direction of the bedding planes) in addition to the

specified excavation and support methods (see Table 4) for better control over the occurrence of overbreak. The minor spalling in some parts of zones 3 and 7 was also observed where the overburden was more than 400 m.

Type C2: The caving in the tunnel roof has happened in type C2 in zones 5 and 7 (see Table 3). In zone 5 the caving happened despite following the excavation and support plan outlined in Table 4, and resulted in approximately two months of delay in the time schedule. The pre-excavation grouting coupled with the spiling proved to be more effective in preventing the caving behavior of the surrounding rock mass, and thus, it is recommended to apply pre-excavation grouting in type C2 especially during the excavation of the Alborz western tunnel (see Table 4).

Type D: Generally the only problem associated with this type was the convergence in the tunnel roof and walls in zone 6. The convergence was overcome by implementation of the final lining with reinforced concrete. Monitoring the loads on the final lining showed that the convergence of the tunnel was under control after the installation of the concrete lining.

Type E: The total encountered length of this type was 34 m in zones 1 and 2 (see Table 5). The squeezing of the rock mass was observed in zone 1 even after installation of the primary support. The rock mass behavior in this section of the tunnel was continuously monitored by convergence tape, load cells, and extensometers. However, after the installation of the concrete lining the convergence was under control.

Type F: This type was used for the tunnel portals regardless of the rock mass type.

The type B was not encountered during the excavation of the Alborz eastern tunnel. The tunnel route was mainly consisted of types C1 and C2 (see Table 5), the behavior of which is controlled by the effect of gravity.

Table 5 The lengths and observed ground behavior types in the Alborz eastern tunnel (The information in zones 1, 2, and 7 were not fully available)

| Zone | Length (m) | | | | | Sum of the lengths (m) | Experienced problems Observed behavior |
|------|------------|------|-----|----|----|------------------------|--|
| | B | C1 | C2 | D | E | | |
| 1 | 0 | 641 | 8 | 9 | 11 | 669 | Rock fall/wedge instability in C1, Squeezing in E |
| 2 | 0 | 177 | 0 | 0 | 23 | 200 | Rock fall in C1 |
| 3 | 0 | 838 | 41 | 71 | 0 | 950 | Rock fall/wedge instability, and Excessive overbreak due to bedding dips in C1 Occasional emissions of CH ₄ and H ₂ S gases all along |
| 4 | 0 | 476 | 54 | 0 | 0 | 530 | Rock fall/wedge instability and buckling in C1 |
| 5 | 0 | 303 | 97 | 0 | 0 | 400 | Caving in C2, rock fall/wedge instability in C1 |
| 6 | 0 | 288 | 143 | 39 | 0 | 470 | Rock fall/wedge instability in C1, radial convergence in D |
| 7 | 0 | 1636 | 404 | 10 | 0 | 2050 | Rock fall/wedge instability in C1, Caving in C2 Emissions of CH ₄ gas all along |

5.2. Continuity factor in the GDE multiple graph

The project-related features such as the opening size can contribute to the rock mass behavior. The continuity factor (CF) defined as excavation diameter/block diameter indicates the number of blocks occurring at the tunnel roof. This factor is an important parameter in the design of underground structures and is defined as below [24]:

- Continuous (massive rock): $CF < 6$
- Discontinuous (blocky): $CF=3-30$
- Continuous (particulate (crushed) rock): $CF>15$

There is an overlap of CF in the ranges of 3-6 and 15-30 where both continuous and discontinuous behavior might happen.

The GDE multiple graph approach uses the block volume in its description of the rock mass behavior (see section 2.1). However, the continuity factor is not taken into account in this method. Thus, a comparison was made between the GBT and GDE in order to determine the continuity in GDE multiple graph classes of rock mass behavior. This comparison provides the continuity factor for each type of rock mass behavior in the GDE multiple graph approach. The results are shown in Figure 3, where only the initial behavior of the rock

mass in the GBT method is considered. Moreover, the buckling behavior in the GBT method depends on the mineral properties of the rock mass and is not covered in the GDE multiple graph.

6. The applicability of RSF

The GDE multiple graph approach is used to determine the applicability range of the RSF (see section 3) based on the information obtained during the construction of the Alborz tunnel. The rock mass along the overall length of the Alborz tunnel was mainly consisted of types C1 and C2 together with some occurrences of types D and E. The histograms of the RSF values obtained from the geological face mappings in each type of rock mass behavior are shown in Figure 4. The details are presented in Table 6. The RSF in rock type C1 (RMR=40-60) has larger range compared to that of types C2 and D. Moreover, it can be seen that in types C2 and D the higher frequencies lie mostly towards the larger RSF values. The reason for this is the presence of infilling material in all joint sets in the rock types C2 and D in the Alborz tunnel. Thus, the rating of the joint condition for the RMR system was conducted directly instead of using the parameters of the joint condition (i.e. joint persistence, surface roughness, aperture, infilling material, and degree of weathering). This is due to the instructions given by Bieniawski to use a direct

rating for the condition of joints where the infilling materials are present [1]. This instruction is in place because the presence of infilling material prevents the occurrence of full contact between the joint walls, which renders the shear resistance of the joint surfaces unlikely to be the prevailing factor contributing to the rock mass behavior. The smaller standard deviation in the RSF values in rock types C2 and D compared to that of rock type C1 (see Table 6) is also due to the direct rating of the joint condition.

The RSF is defined as an indicator of the capability of the rock mass to be enhanced by rock bolting in terms of the shear resistance of its joint sets. The shear resistance of the joint walls against any movement is the key point in the definition of RSF. Thus, in the rock types C2 and D where the directly assigned joint condition rating does not account for the shear resistance of the joints, the

application of RSF is not valid. In general, the rock mass behavior is not considerably determined by the shear resistance of the joint sets in rock types C2 and D as both are continuous (particulate or crushed) rocks. The support system designated for these rock types where the lattice girders act as the main element of the support preventing the possible occurrence of caving or plastic behavior (see Table 4) also indicate that the shear resistance of the joint surfaces is not the main factor. Moreover, in rock types A, B, C1 (RMR=60-80), C3, and C4 where the rock type is continuous (massive rock) the rock mass behavior does not depend on the shear resistance of the joint surfaces. This leaves the rock type C1 (RMR=40-60), i.e. the discontinuous rock, where the behavior of the rock mass is mostly determined by the joint condition as the only type in which the application of the RSF is valid.

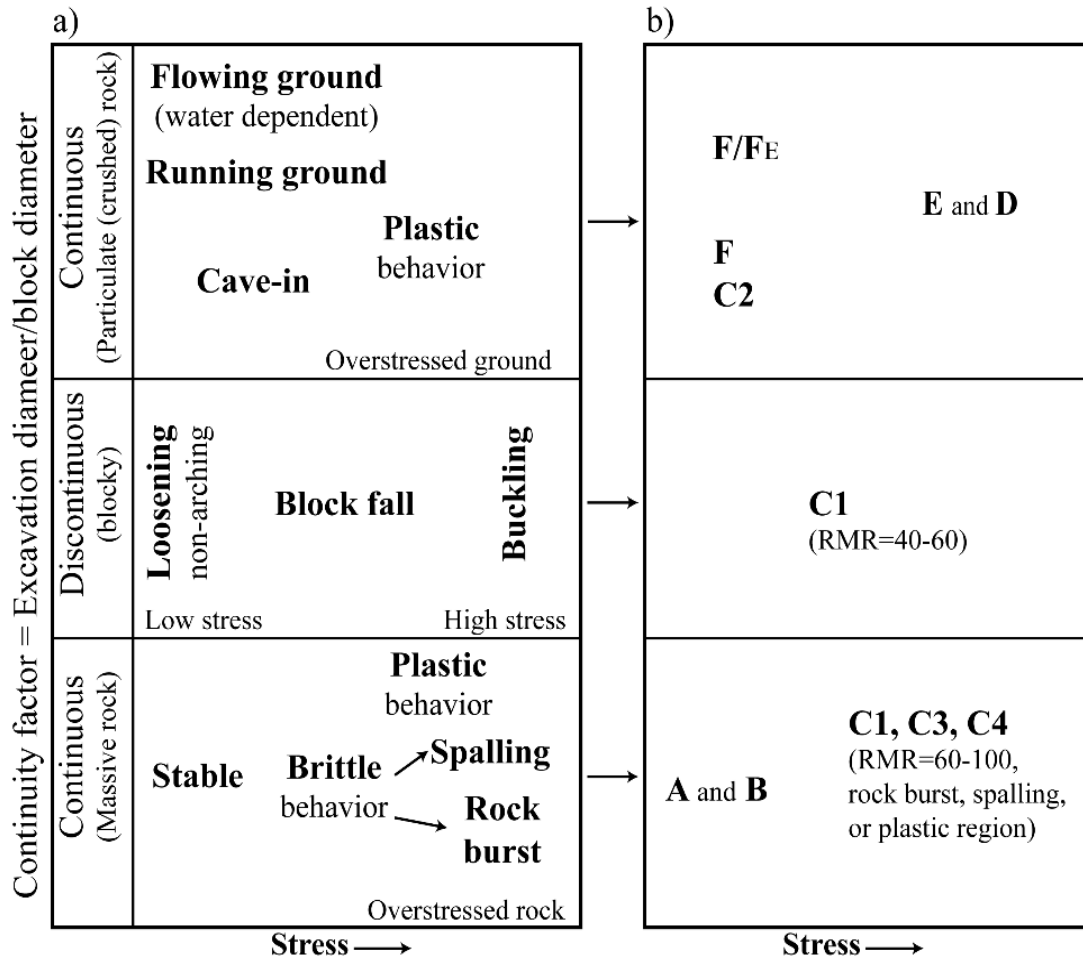


Figure 3. a) The initial behavior of rock mass based on the GBT b) The continuity factor developed for rock mass behavior classes of GDE multiple graph

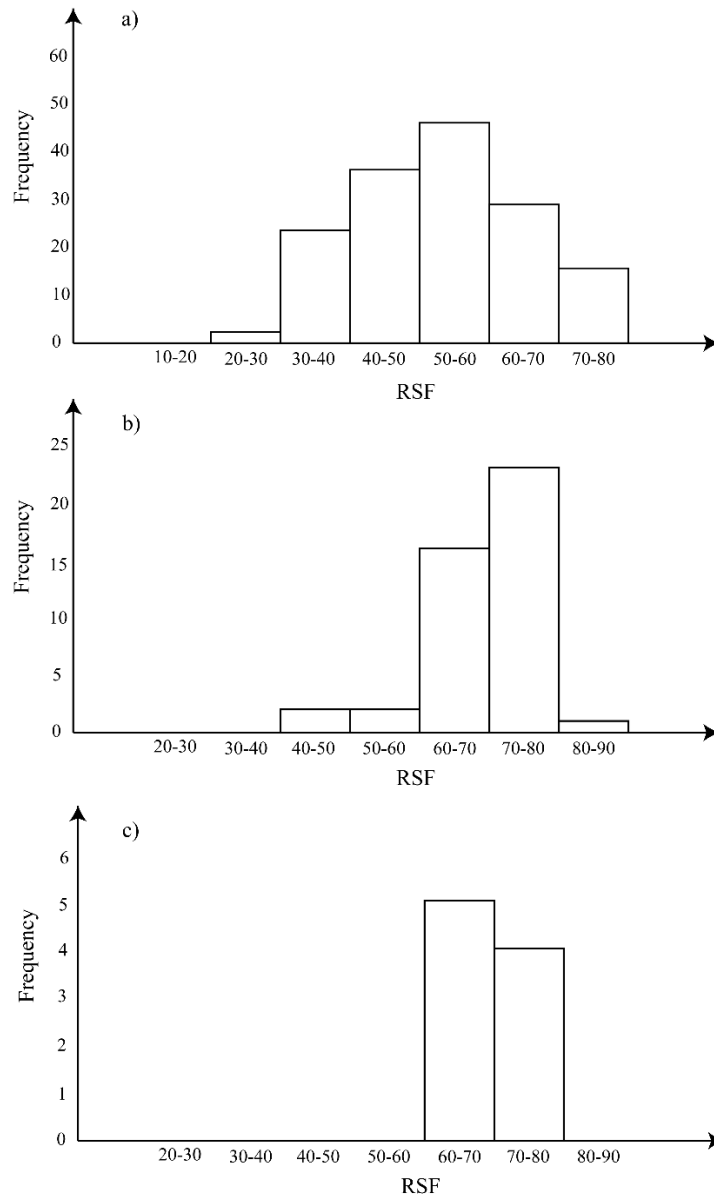


Figure 4. a) The distribution of RSF values for rock type C1 (RMR=40-60) in the Alborz tunnel b) The distribution of RSF values for rock type C2 in the Alborz tunnel c) The distribution of RSF values for rock type D in the Alborz tunnel

Table 6. The RSF calculation details in rock types C1, C2, and D in the Alborz tunnel

| GDE rock class | Total number of face mappings | Rock mass continuity | RSF | |
|----------------|-------------------------------|----------------------|------------|--------------------|
| | | | Mean value | Standard deviation |
| C1 | 151 | Discontinuous | 55 | 12 |
| C2 | 44 | Continuous | 70 | 11 |
| D | 9 | Continuous | 70 | 4 |

The relationship between the RMR and RSF in type C1 (RMR=40-60) of rock mass behavior is shown in Figure 5 for the data obtained from the excavation of the Alborz tunnel (151 geological face mappings). A negative correlation exists between the RMR and RSF values where the correlation coefficient is -0.39. The relatively small

correlation coefficient between the RMR and RSF implies that for the type C1 (RMR=40-60) of rock mass behavior the RSF value is not strictly dependent on the RMR value. This is because of the definition of the RSF, which is based on the rating of the joint condition in the RMR system where similar RMR values can have different joint

conditions. In fact, the weak correlation indicates that the RSF can be a useful tool in the explanation of the differences among the rock masses with the same RMR values that belong to the behavioral type C1 of the GDE multiple graph or discontinuous (blocky) rock mass (see also Figure 3).

The combination of the rock mass and the rock bolts can be considered as an equivalent rock mass [29, 38]; where an equivalent RMR value, i.e. RMR_{eq} , can be calculated from Equation 3. The RMR_{eq} values in rock type C1 are calculated for the dataset from the Alborz tunnel and plotted against the RMR values in Figure 6. The RMR_{eq} in the majority of the cases are higher than 60 which means that the rock bolting improved the rock mass class in the RMR system. The shift from the $RMR_{eq} = RMR$ line visually demonstrates the effect of rock bolting in improvement of the RMR value of rock mass. This fact can be used in the application of the RMR values for designing a support system, calculating rock mass properties, or calculating the total load on the support system. Thus, the RSF can be a useful tool for incorporating the effect of rock bolting in the design of

underground structures in discontinuous (blocky) rock masses. The calculation of the RSF does not require extra information and investigations if the ratings of the joint condition parameter of the RMR system are available. Thus, it is very easy to obtain the RSF values.

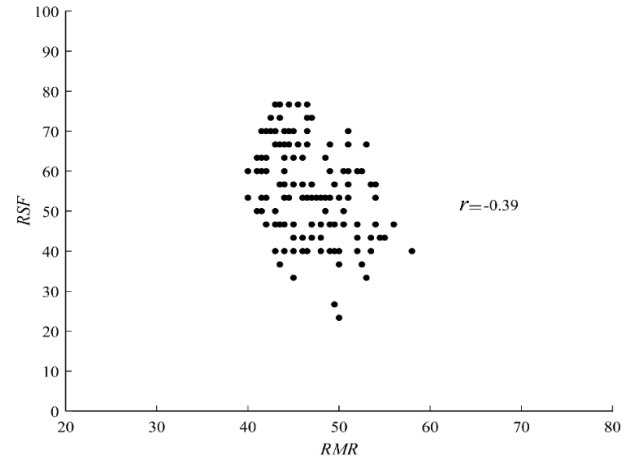


Figure 5. RSF versus RMR in rock class C1 of the GDE multiple graph approach in the Alborz tunnel based on 151 face mappings

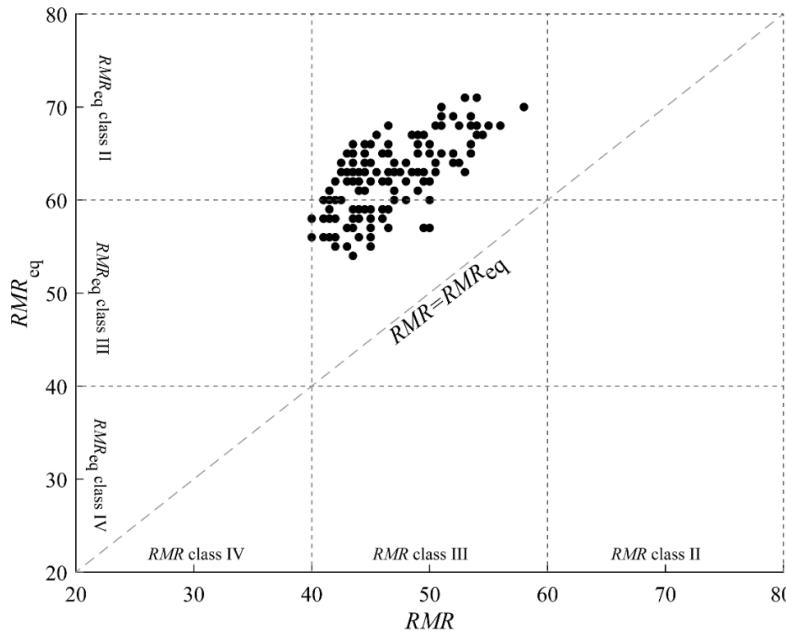


Figure 6. RMR_{eq} versus RMR in rock class C1 of the GDE multiple graph approach in the Alborz tunnel

7. Conclusions

It is of paramount importance to understand the behavior of rock mass for the design and construction of underground structures in rock. The rock mass behavior can be determined and described based on the GDE multiple graph approach and the GBT method. The experience

gained from the construction of the Alborz tunnel in Iran with regard to the application of the GDE multiple graph approach is presented in this paper. In addition, the GDE and GBT methods are compared in terms of their classification of the rock mass behavior and the continuity factor of the GBT method is assigned for the GDE method. As a

result, a system is developed that covers the gap concerning rock mass continuity factor in application of the GDE multiple graph approach for prediction rock mass behavior. This system helps determine the applicability of the RSF concept in different rock types. Using the system together with the geological face mapping data from the Alborz tunnel it is concluded that the RSF is only applicable in the rock mass type C1 where the RMR values ranges from 41 to 60. The usefulness of the RSF in design and construction of underground structures is discussed by using the data from the Alborz tunnel.

References

- [1]. Bieniawski, Z. T. (1989). *Engineering rock mass classifications: a complete manual for engineers and geologists in mining, civil, and petroleum engineering*. John Wiley & Sons.
- [2]. Barton, N., Lien, R., & Lunde, J. J. R. M. (1974). Engineering classification of rock masses for the design of tunnel support. *Rock mechanics*, 6, 189-236.
- [3]. Bieniawski, Z. T. (1973). Engineering classification of jointed rock masses. *Civil Engineering= Sivielle Ingenieurswese*, 1973(12), 335-343.
- [4]. Deere, D. U., Hendron, A. J., Patton, F. D., & Cording, E. J. (1966, September). Design of surface and near-surface construction in rock. In *ARMA US Rock Mechanics/Geomechanics Symposium* (pp. ARMA-66). ARMA.
- [5]. Hoek, E., Kaiser, P. K., & Bawden, W. F. (2000). *Support of underground excavations in hard rock*. CRC Press.
- [6]. Lauffer, H. (1958). Classification for tunnel construction. *Geologie und Bauwesen*, 24(1), 46-51.
- [7]. Palmström, A. (1996). Characterizing rock masses by the R_{Mi} for use in practical rock engineering: Part 1: The development of the Rock Mass index (R_{Mi}). *Tunnelling and underground space technology*, 11(2), 175-188.
- [8]. Palmström, A. (1996). Characterizing rock masses by the R_{Mi} for use in practical rock engineering, part 2: some practical applications of the rock mass index (R_{Mi}). *Tunnelling and underground space technology*, 11(3), 287-303.
- [9]. Terzaghi, K. (1946). Rock defects and loads on tunnel supports. *Rock tunneling with steel supports*.
- [10]. Wickham, G. E., Tiedemann, H. R., & Skinner, E. H. (1972, June). Support determinations based on geologic predictions. In *N Am Rapid Excav & Tunnelling Conf Proc* (Vol. 1).
- [11]. Aydan, Ö., Ulusay, R., & Tokashiki, N. (2014). A new rock mass quality rating system: rock mass quality rating (RMQR) and its application to the estimation of geomechanical characteristics of rock masses. *Rock mechanics and rock engineering*, 47, 1255-1276.
- [12]. Bar, N., & Barton, N. (2017). The Q-slope method for rock slope engineering. *Rock Mechanics and Rock Engineering*, 50, 3307-3322.
- [13]. Barton, N., & Bar, N. (2019, September). The Q-slope method for rock slope engineering in faulted rocks and fault zones. In *ISRM Congress* (pp. ISRM-14CONGRESS). ISRM.
- [14]. Hoek, E., Carter, T. G., & Diederichs, M. S. (2013, June). Quantification of the geological strength index chart. In *ARMA US Rock Mechanics/Geomechanics Symposium* (pp. ARMA-2013). ARMA.
- [15]. Laubscher, D. H., & Jakubec, J. (2001). The MRMR rock mass classification for Jointed Rock Masses. *Underground mining methods: engineering fundamentals and international case studies*, 475-481.
- [16]. Maazallahi, V., & Majdi, A. (2021). Directional rock mass rating (DRMR) for anisotropic rock mass characterization. *Bulletin of Engineering Geology and the Environment*, 80, 4471-4499.
- [17]. Marinos, V. (2019). A revised, geotechnical classification GSI system for tectonically disturbed heterogeneous rock masses, such as flysch. *Bulletin of Engineering Geology and the Environment*, 78, 899-912.
- [18]. Mohammadi, M. (2021, October). Application of Rock Mass Rating system in underground intersections. In *IOP Conference Series: Earth and Environmental Science* (Vol. 861, No. 5, p. 052081). IOP Publishing.
- [19]. Saroglou, C., Qi, S., Guo, S., & Wu, F. (2019). ARMR, a new classification system for the rating of anisotropic rock masses. *Bulletin of Engineering Geology and the Environment*, 78, 3611-3626.
- [20]. Sonmez, H., & Ulusay, R. (1999). Modifications to the geological strength index (GSI) and their applicability to stability of slopes. *International Journal of Rock Mechanics and Mining Sciences*, 36(6), 743-760.
- [21]. Rezaei, M., & Habibi, H. (2023). Designing of the Beheshtabad water transmission tunnel based on the hybrid empirical method. *Structural Engineering and Mechanics*, 86(5), 621-633.
- [22]. Palmstrom, A., & Stille, H. (2007). Ground behaviour and rock engineering tools for underground excavations. *Tunnelling and Underground Space Technology*, 22(4), 363-376.
- [23]. Stille, H., & Palmström, A. (2003). Classification as a tool in rock engineering. *Tunnelling and underground space technology*, 18(4), 331-345.
- [24]. Stille, H., & Palmström, A. (2008). Ground behaviour and rock mass composition in underground excavations. *Tunnelling and Underground Space*

Technology, 23(1), 46-64.

[25]. Russo, G., & Grasso, P. (2007, July). On the classification of the rock mass excavation behaviour in tunneling. In *ISRM Congress* (pp. ISRM-11CONGRESS). ISRM.

[26]. Russo, G. (2008). A simplified rational approach for the preliminary assessment of the excavation behaviour in rock tunnelling. *Tunnels et ouvrages souterrains*, 207(May-June).

[27]. Russo, G. (2014). An update of the “multiple graph” approach for the preliminary assessment of the excavation behaviour in rock tunnelling. *Tunnelling and underground space technology*, 41, 74-81.

[28]. Russo, G. (2014). An update of the “multiple graph” approach for the preliminary assessment of the excavation behaviour in rock tunnelling. *Tunnelling and underground space technology*, 41, 74-81.

[29]. Mohammadi, M., Hossaini, M. F., & Bagloo, H. (2017). Rock bolt supporting factor: rock bolting capability of rock mass. *Bulletin of engineering geology and the environment*, 76, 231-239.

[30]. Mohammadi, M., & Hossaini, M. F. (2017). Modification of rock mass rating system: Interbedding of strong and weak rock layers. *Journal of rock mechanics and geotechnical engineering*, 9(6), 1165-1170.

[31]. Antolović, M., Filipović, A., & Amadini, F. (2013). Engineering geological behaviour of rock mass in Chenani-Nashri tunnel, the longest Road tunnel in

India. In *Tunnelling in Mediterranean Region*.

[32]. Decman, A., Stella, F., & Verzani, L. P. (2013, May). Geomechanical follow-up of El Teniente new mine level access tunnels. ITA symposium Croatia.

[33]. Palomba, M., Russo, G., Amadini, F., Carrieri, G., & Jain, A. R. (2013, May). Chenani-Nashri Tunnel, the longest road tunnel in India: a challenging case for design-optimization during construction. In *World Tunnel Congress 2013. Underground-the way to the future* (pp. 964-971).

[34]. Kontrec, P., & Constandinidis, V. (2013, May). Engineering geological characterization of the rock mass in the Adit P4600. In *Project El Teniente, Chile, ITA symposium Croatia* (pp. 7-8).

[35]. Mohammad, S., Hossaini, F., Mohammadi, M., & Askari, M. (2018). Interpretation of Rock Mass Behaviour via "Multiple Graph" Approach: Adit P-C9 of the Alborz Tunnel.

[36]. Habenicht, H. (2021). The anchoring effects—Our present knowledge and its shortcomings: A keynote lecture. *Rock bolting: Theory and application in mining and underground construction*, 257-268.

[37]. Tehran-Shomal Freeway Co. (2018), “Detailed reports and maps of Alborz tunnel,,” Tehran, Iran.

[38]. Stille, H., Holmberg, M., & Nord, G. (1989, January). Support of weak rock with grouted bolts and shotcrete. In *International Journal of Rock Mechanics and Mining Sciences & Geomechanics Abstracts* (Vol. 26, No. 1, pp. 99-113). Pergamon.

کاربرد شاخص راکبولت خوری سنگ (RSF) بر اساس رفتار توده سنگ؛ مطالعه موردی تونل البرز

حامد فرج الهی^۱، محمد محمدی^۲ و محمدحسین خسروی^{۳*}

۱- دانشکده مهندسی معدن، پردیس دانشکدگان فنی، دانشگاه تهران، تهران، ایران

۲- بخش مکانیک خاک و سنگ، موسسه سلطنتی فناوری KTH، استکهلم، سوئد

۳- گروه مهندس معدن، دانشکده مهندسی، دانشگاه بیرجند، بیرجند، ایران

ارسال ۲۰۲۴/۰۴/۰۸، پذیرش ۲۰۲۴/۰۸/۳۰

* نویسنده مسئول مکاتبات: mh.khosravi@birjand.ac.ir

چکیده:

رسیدن به درک بهتر از رفتار توده سنگ بخش اساسی طراحی و ساخت سازه‌های زیرزمینی است. هرگونه بهبود در درک رفتار توده سنگ، بهبود طراحی را از نظر ایمنی محیط کار، ایمنی طولانی مدت سازه، اثرات زیست محیطی و مدیریت صحیح منابع عمومی یا خصوصی تسهیل می‌کند. بنابراین، در گام اول این مقاله، تجربه به دست آمده از استفاده از روش نمودار چندگانه GDE (مهندسی داده‌های جغرافیایی) برای طبقه‌بندی توده سنگ و ارزیابی رفتار آن در طول حفاری تونل البرز ارائه شده است. خطرات پیش‌بینی شده با مشکلات تجربه شده مقایسه شده و پیشنهاداتی برای بررسی در کارهای آتی ساخت تونل ارائه شده است. در گام دوم، روش نمودار چندگانه GDE با انواع رفتار توده سنگ پیشنهاد شده توسط پالمسروم و استیل (۲۰۰۷)، از نظر پیوستگی توده سنگ مقایسه شده است. نتیجه این مقایسه همراه با داده‌های به دست آمده از طبقه‌بندی توده سنگ در تونل البرز برای توسعه سیستمی استفاده می‌شود که کاربرد شاخص راکبولت خوری سنگ (RSF) را در کلاس‌های رفتاری مختلف توده سنگ تعیین می‌کند.

کلمات کلیدی: رفتار توده سنگ، نمودار چندگانه GDE؛ سیستم طبقه‌بندی توده سنگ (RMR)؛ شاخص راکبولت خوری سنگ (RSF)؛ تونل البرز.